Superconductivity at the Two-Dimensional Limit

Shengyong Qin *et al.*

Science **324**, 1314 (2009);
DOI: 10.1126/science.1170775

Science (print ISSN 0036-8075; online ISSN 1095-9203) is published weekly, except the last week in December, by the American Association for the Advancement of Science, 1200 New York Avenue NW, Washington, DC 20005.

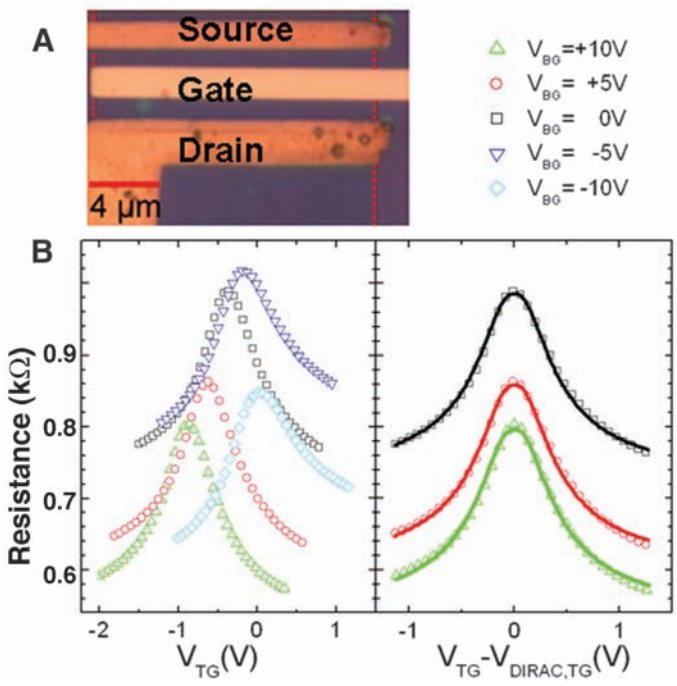

Fig. 3. (**A**) Optical microscope image of a graphene FET. (**B**) Device resistance versus top-gate voltage (V_{TG}), with different back-gate (V_{BG}) biases, and versus V_{TG}-$V_{Dirac,TG}$ (V_{TG} at the Dirac point), with a model fit (solid line).

much less than 10 min, the Cu surface is usually not fully covered [SEM images of graphene on Cu with different growth time are shown in fig. S3 (*15*)]. The growth of graphene on Cu foils of varying thickness (12.5, 25, and 50 μm) also yielded similar graphene structure with regions of double and triple flakes, but neither discontinuous monolayer graphene for thinner Cu foils nor continuous multilayer graphene for thicker Cu foils, as we would have expected based on the precipitation mechanism. According to these observations, we concluded that graphene is growing by a surface-catalyzed process rather than a precipitation process, as has been reported by others for Ni (*5*–*7*). Monolayer graphene formation caused by surface segregation or surface adsorption of carbon has also been observed on transition metals such as Ni and Co at elevated temperatures by Blakely and coauthors (*20*–*22*). However, when the metal substrates were cooled down to room temperature, thick graphite films were obtained because of precipitation of excess C from these metals, in which the solubility of C is relatively high.

In recent work, thin Ni films and a fast-cooling process have been used to suppress the amount of precipitated C. However, this process still yields films with a wide range of graphene layer thicknesses, from one to a few tens of layers and with defects associated with fast cooling (*5*–*7*). Our results suggest that the graphene growth process is not one of C precipitation but rather a CVD process. The precise mechanism will require additional experiments to understand in full, but very low C solubility in Cu (*23*–*25*) and poor C saturation as a result of graphene surface coverage may be playing a role in limiting or preventing the precipitation process altogether at high temperature, similar to the case of impeding of carburization of Ni (*26*). This provides a pathway for growing self-limited graphene films.

To evaluate the electrical quality of the synthesized graphene, we fabricated dual-gated FETs with Al_2O_3 as the gate dielectric and measured them at room temperature. Along with a device model that incorporates a finite density at the Dirac point, the dielectric, and the quantum capacitances (*9*), the data are shown in Fig. 3. The extracted carrier mobility for this device is ~4050 $cm^2\ V^{-1}\ s^{-1}$, with the residual carrier concentration at the Dirac point of $n_0 = 3.2 \times 10^{11}\ cm^{-2}$. These data suggest that the films are of reasonable quality, at least sufficient to continue improving the growth process to achieve a material quality equivalent to the exfoliated natural graphite.

References and Notes

1. A. K. Geim, K. S. Novoselov, *Nat. Mater.* **6**, 183 (2007).
2. C. Berger *et al.*, *Science* **312**, 1191 (2006); published online 12 April 2006 (10.1126/science.1125925).
3. K. V. Emtsev *et al.*, *Nat. Mater.* **8**, 203 (2009).
4. P. W. Sutter, J.-I. Flege, E. A. Sutter, *Nat. Mater.* **7**, 406 (2008).
5. Q. Yu *et al.*, *Appl. Phys. Lett.* **93**, 113103 (2008).
6. K. S. Kim *et al.*, *Nature* **457**, 706 (2009).
7. A. Reina *et al.*, *Nano Lett.* **9**, 30 (2009).
8. J. Coraux, A. T. N'Diaye, C. Busse, T. Michely, *Nano Lett.* **8**, 565 (2008).
9. S. Kim *et al.*, *Appl. Phys. Lett.* **94**, 062107 (2009).
10. M. C. Lemme *et al.*, *Solid-State Electron.* **52**, 514 (2008).
11. S. K. Banerjee, L. F. Register, E. Tutuc, D. Reddy, A. H. MacDonald, *IEEE Electron Device Lett.* **30**, 158 (2009).
12. P. Blake *et al.*, *Nano Lett.* **8**, 1704 (2008).
13. R. R. Nair *et al.*, *Science* **320**, 1308 (2008); published online 3 April 2008 (10.1126/science.1156965).
14. X. Wang, L. Zhi, K. Müllen, *Nano Lett.* **8**, 323 (2008).
15. See supporting material on *Science* Online.
16. A. Reina *et al.*, *J. Phys. Chem. C* **112**, 17741 (2008).
17. Z. H. Ni *et al.*, *Nano Lett.* **7**, 2758 (2007).
18. A. C. Ferrari *et al.*, *Phys. Rev. Lett.* **97**, 187401 (2006).
19. A. Das *et al.*, *Nat. Nanotechnol.* **3**, 210 (2008).
20. M. Eizenberg, J. M. Blakely, *Surf. Sci.* **82**, 228 (1979).
21. M. Eizenberg, J. M. Blakely, *J. Chem. Phys.* **71**, 3467 (1979).
22. J. C. Hamilton, J. M. Blakely, *Surf. Sci.* **91**, 199 (1980).
23. R. B. McLellan, *Scr. Metal.* **3**, 389 (1969).
24. G. Mathieu, S. Guiot, J. Carbané, *Scr. Metal.* **7**, 421 (1973).
25. G. A. López, E. J. Mittemeijer, *Scr. Mater.* **51**, 1 (2004).
26. R. Kikowatz, K. Flad, G. Horz, *J. Vac. Sci. Technol. A* **5**, 1009 (1987).

27. We thank the Nanoelectronic Research Initiative (NRI–Southwest Area Nanoelectronics Center, grant no. 2006-NE-1464), the Defense Advanced Research Projects Agency Carbon Electronics for RF Applications Center, and the University of Texas at Austin for support.

Supporting Online Material

www.sciencemag.org/cgi/content/full/1171245/DC1
Materials and Methods
Figs. S1 to S3

22 January 2009; accepted 9 April 2009
Published online 7 May 2009;
10.1126/science.1171245
Include this information when citing this paper.

Superconductivity at the Two-Dimensional Limit

Shengyong Qin, Jungdae Kim, Qian Niu, Chih-Kang Shih*

Superconductivity in the extreme two-dimensional limit is studied on ultrathin lead films down to two atomic layers, where only a single channel of quantum well states exists. Scanning tunneling spectroscopy reveals that local superconducting order remains robust until two atomic layers, where the transition temperature abruptly plunges to a lower value, depending sensitively on the exact atomic structure of the film. Our result shows that Cooper pairs can still form in the last two-dimensional channel of electron states, although their binding is strongly affected by the substrate.

Studies of two-dimensional (2D) superconductivities have been generally limited to the regime where the superconducting order parameter behaves as a 2D wave function but the underline electrons are still three-dimensional (*1*–*11*). Recent advancements in materials synthesis have enabled the growth of epitaxial superconductor thin films with unprec-

edented control in crystallinity, atomic smoothness, and film thickness, thus opening up new opportunities in investigations of 2D superconductivity (*7*–*16*). Studies of superconducting properties of ultrathin Pb films on Si or Ge substrates by transport, magnetic, and spectroscopic measurements have revealed several new aspects of 2D superconductivity (*7*–*11*), such as quantum oscillations of the superconducting order parameter as a function of the film thickness (*7*, *8*). Moreover, D. Eom *et al*. discovered that superconductivity remains surprisingly robust, even for films as thin as 5 monolayers (ML) (*8*). However, even in such thin films, there still exist several quantum well channels (*17*). It is unclear how much mixing between them occurs and how such mixing influences superconductivity. Consequently, some very interesting questions arise: Could it be possible to engineer a superconducting thin film with only one quantum well channel? Moreover, what will be the superconducting properties at this ultimate limit, and in particular, to what extent does the robustness of superconductivity remain at this limit?

The transition temperature (T_c) as a function of the film thickness (Fig. 1) shows oscillations for $L > 5$ (where L is the number of atomic layers) that have been reported previously, as well as new data for the thinnest films down to $L = 2$, which is the last Pb film that can be stable according to the quantum growth principle (*18*). More notably, $L = 2$ also corresponds to the single quantum channel regime: Along the (111) crystal direction, $k_F = 0.45\ \pi/d$, where k_F is the Fermi wave vector, and d is the spacing between lattice planes, giving rise to the condition of $k_F L \sim \pi$ for the existence of a single quantum well channel. As the film thickness decreases, one first observes an increase of the quantum oscillations of T_c, followed by a dramatic drop of T_c to substantially lower values at the ultimate limit of 2 ML. In addition, we find that there are two different types of $L = 2$ films, which differ in subtle atomic reconstructions but have a substantial difference in T_c.

The fabrication of pristine ultrathin films requires a careful preparation of the substrate, resulting in a Pb-Si reconstruction template containing a mixture of $\sqrt{3}\times\sqrt{3}$ and $\sqrt{7}\times\sqrt{3}$ structures (fig. S1) (*19*–*22*). This procedure results in a uniform 2-ML Pb film on the template (Fig. 2A). There are two types of 2-ML Pb films (labeled as type I and II); each type resides on an individual terrace. A zoom-in view shows that type I has an underlying 1 × 1 atomic structure with a moiré pattern periodicity of ~3.0 nm (Fig. 2B), whereas type II has an underlying $\sqrt{3} \times \sqrt{3}$ atomic structure (oriented 30° with respect to the 1 × 1 structure) with a moiré pattern periodicity of ~4.4 nm (Fig. 2C). Moreover, the underlying 1 × 1 structure in type I has the same surface lattice parameter (3.50 ± 0.10 Å) as the bulk Pb to within 3%, whereas the $\sqrt{3} \times \sqrt{3}$ structure in type II has a lattice parameter of 6.50 ± 0.15 Å, which is very close to that of the Si $\sqrt{3}\times\sqrt{3}$ structure, implying the existence of a pseudomorphic strain.

Although in this image, type I is more abundant, investigations over more than 100 terraces show that there is no preferential abundance of either type. Most notably, we never observe a mixed phase of type I and II on the same terrace. Often, type II contains small holes of 2- to 6-nm in diameter that extend down to the substrate. On type I film, however, holes are formed at the descending edge of the terrace. Such holes ex-

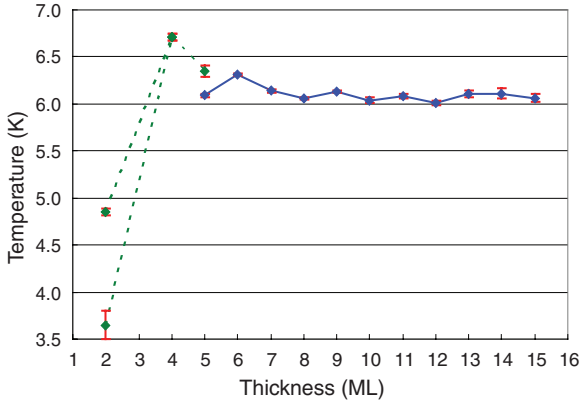

Fig. 1. Superconducting transition temperature (T_c) as a function of film thickness. As the film thickness decreases, an increase of the quantum oscillations of T_c was observed, followed by a dramatic drop of T_c to substantially lower values at the ultimate limit of 2 ML. At $L = 2$, two different kinds of films result in two different T_c values. The data point at $L = 3$ is absent because it is thermodynamically unstable to form a film of 3 ML. The old data (*8*) were acquired on films grown on Si(111) 7 × 7, whereas the new data (2, 4, and 5 ML) were acquired on films grown on a new Pb-Si(111) template. Determination of T_c and error bars are described in the supporting online material.

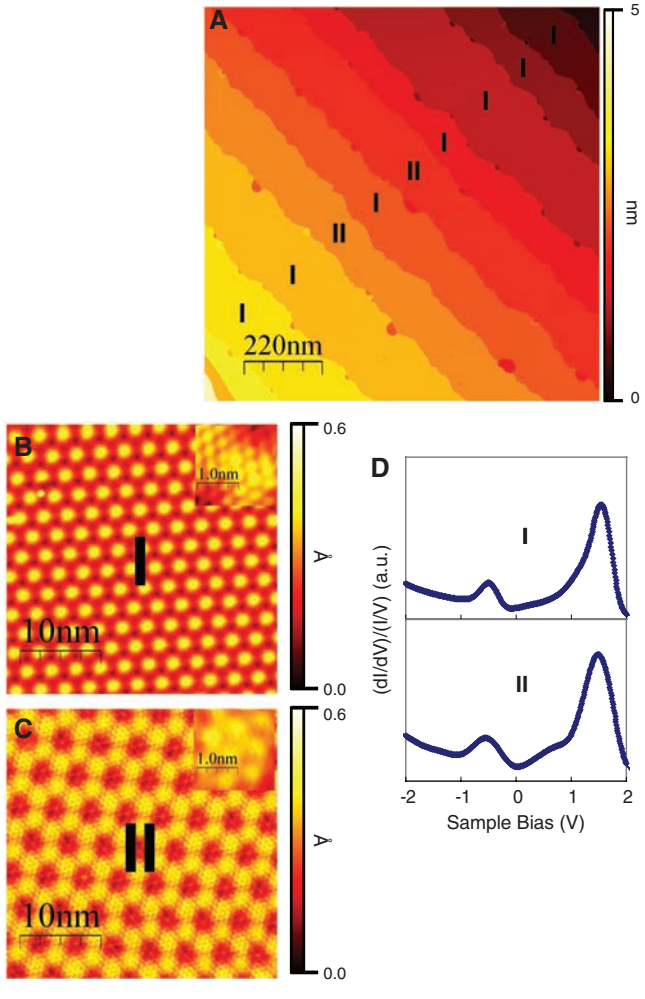

Fig. 2. (**A**) STM image of a uniform 2-ML Pb film. (**B** and **C**) STM images of two types of 2-ML Pb films (labeled as type I and II); each type resides on an individual terrace. Insets are zoom-in views, showing that type I has an underlying 1 × 1 atomic structure with a moiré pattern periodicity of ~3.0 nm (B), whereas type II has an underlying $\sqrt{3} \times \sqrt{3}$ atomic structure with a moiré pattern periodicity of ~4.4 nm (C). The orientation of the $\sqrt{3} \times \sqrt{3}$ atomic structure is rotated 30° with respect to the 1 × 1 structure. (**D**) Tunneling spectroscopy of QWS on two types of films, revealing the same level spacing and relative positions to E_F. a.u., arbitrary units.

Department of Physics, The University of Texas at Austin, Austin, TX 78712, USA.

*To whom correspondence should be addressed. E-mail: shih@physics.utexas.edu

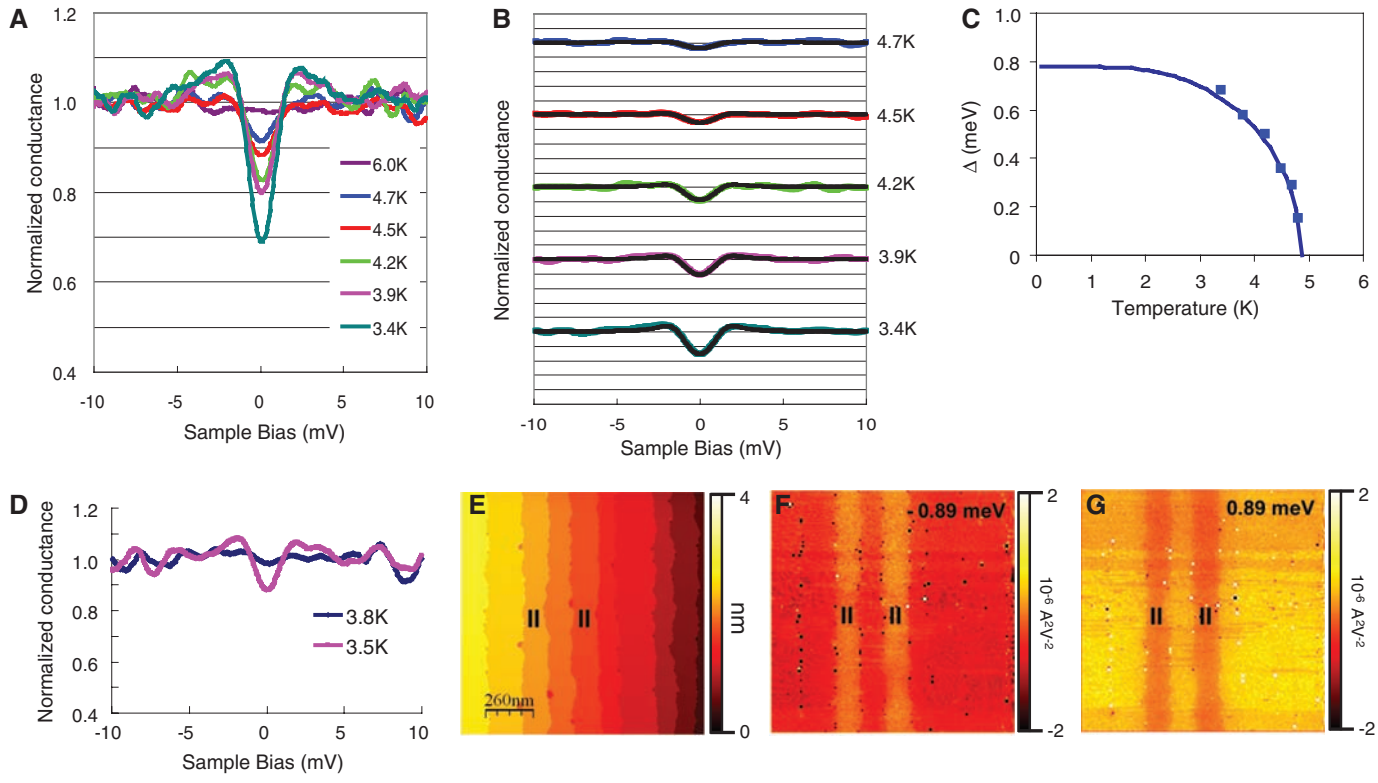

Fig. 3. (**A**) Normalized conductance spectra acquired at various temperatures for type I films. The superconducting gap is clearly visible at 3.4 K and gradually disappears as the temperature is raised to 6.0 K. (**B**) Normalized conductance spectra (nonblack colors) taken by STM were fitted using the BCS-like formula for the tunneling conductance (black). (**C**) The energy gaps (Δ) for several temperatures were obtained from (B) and plotted as blue squares. The blue curve is a fitting of these energy gap data using a BCS-like gap equation to obtain a T_c of ~4.9 K for the type I film. (**D**) Tunneling measurements of the type II 2-ML films. The superconducting gap did not show until the temperature dropped to 3.5 K. We estimated the T_c to be ~3.65 ± 0.15 K. (**E**) Large-area STM image of 2-ML Pb film. The two terraces labeled with "II" are type II films, and the rest of the terraces are type I. (**F** and **G**) d^2I/dV^2 mapping at 4.0 K (128 × 128 pixels with a pixel resolution of 10.1 nm) at sample biases of –0.89 and 0.89 mV, respectively. First, a large superconductivity contrast between type I and II films was revealed; next, the superconductivity on the same terrace was shown to be very uniform, with clear boundaries at the terrace edges.

pose the substrate template atomic structure, and they allow one to conveniently determine the thickness of the film.

Despite this structural difference, these two types of 2-ML films have almost identical electronic structure in the normal state (*23*). Tunneling spectroscopy (Fig. 2D) reveals the same quantum well states (QWS) level spacing and relative positions to the Fermi level (E_F). This result indicates that the electron density is similar for the two types of films, implying a similar atom density. However, such measurements are not sensitive enough to tell if there is a small difference (i.e., a few percent) in electron density between these two structures.

The superconducting properties of these two types of films, on the other hand, are different. Figure 3A shows tunneling spectra acquired at various temperatures for type I films. The superconducting gap is clearly visible at 3.4 K and gradually disappears as the temperature is raised to 6.0 K. These spectra can be fitted with the Bardeen-Cooper-Schrieffer (BCS)–like density of states (DOS) to obtain a temperature-dependent superconducting gap Δ(T), which allows us to obtain a T_c of ~4.9 K for the type I film (*19*, *24*). However, tunneling measurements of the type II film (Fig. 3C) did not show any superconducting gap until the temperature drops to 3.5 K, at which point a small gap is observed. Because the T_c is very close to the lower temperature limit of our scanning tunneling microscopy (STM), we did not measure enough temperature-dependent data points to fit for the T_c value. Nevertheless, we estimated the T_c to be ~3.65 ± 0.15 K.

To further illustrate spatial variation of the superconducting property, we plotted the 2D mapping of the second derivative of the current-voltage (I-V) curve near the steepest slope of the gap-opening regions. Figure 3E shows a large-area STM image, and Fig. 3, F and G, shows d^2I/dV^2 mapping at biases of –0.89 and 0.89 mV, respectively. Not only does such a second derivative spectroscopic image reveal the large superconductivity contrast between type I and II films, but also it further shows that superconductivity on the same terrace is very uniform, with clear boundaries at the terrace edges.

On such films, one can occasionally find a local region containing coexistence of 4 and 5 ML (Fig. 4A), which allows us to probe the transition region from the ultimate 2-ML limit to thicker regimes that have previously been investigated. On the same sample (and on several subsequently prepared samples), we were not able to find any region with 3-ML film. Even 4-ML regions are quite rare and only can be found when they are connected to 5-ML regions. We take these results as indication of thermodynamic instability at these film thicknesses due to quantum size effect, a subject of extensive investigation in recent years (*12*–*18*). The findings here are consistent with earlier studies, except that they are in an even thinner regime.

The temperature-dependent normalized conductance spectra acquired on 4- and 5-ML films (Fig. 4B) clearly show that the gap in 4-ML films is always deeper than that in 5-ML films at all temperatures. Using the same fitting method, we get the temperature-dependent gap Δ(T), which was fitted with BCS theory, and we were able to obtain a T_c value of 6.7 K for the 4-ML film and 6.3 K for the 5-ML film (Fig. 4C). The contrast in T_c between 4- and 5-ML films illustrates the continuation of the quantum oscillations in the superconducting gap reported earlier, except that here the oscillation amplitude is further enhanced in the thinner regime (Fig. 1).

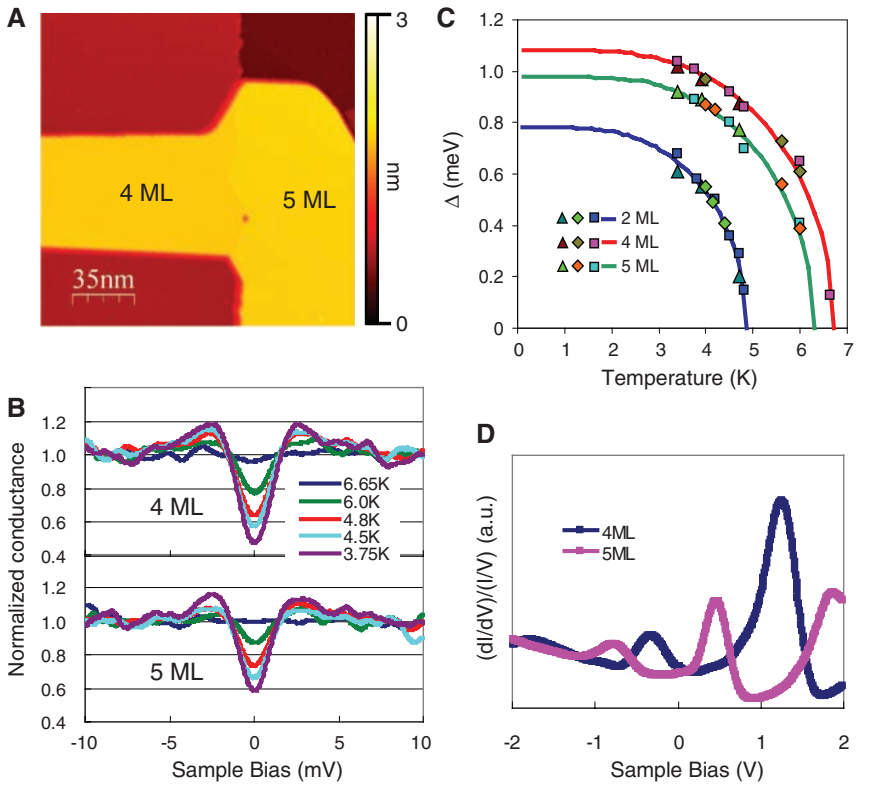

Fig. 4. (**A**) STM image of 4- and 5-ML films. (**B**) Temperature-dependent normalized conductance spectra acquired on 4- and 5-ML films. The gap in 4-ML film is always deeper than that of 5-ML film at all temperatures. (**C**) Fitting with BCS temperature-dependent superconducting gap $\Delta(T)$ for 4- and 5-ML and type I 2-ML films. The data consist of results from three independent runs and are labeled with different symbols. T_c values of 6.7 K for the 4-ML film and 6.3 K for the 5-ML film were obtained. (**D**) Tunneling spectra with a larger bias range acquired above T_c for 4- and 5-ML regions, showing QWS.

Consistent with this interpretation are the locations of the QWS of these two thicknesses (Fig. 4D), where one observes that 4-ML films contain a QWS peak closer to E_F.

Theoretically, a simple jellium model predicts that quantum oscillations of the DOS (and, thus, many electronic properties) would increase in amplitude toward thinner thicknesses (*17*). It is interesting to see that quantum oscillations of the T_c follow the same trend. This trend persists down to 4-ML films where two quantum channels still exist. However, such a robust superconducting behavior takes a substantial dive at 2 ML when only one quantum channel exists.

The observation of persistent superconductivity in all but the last stable film (2-ML film), as shown in Fig. 1, is in sharp contrast with results obtained from transport and magnetic susceptibility studies (*7*, *9*). Starting from large film thicknesses, T_c shows an overall decreasing trend with the thinning of film thickness. In these studies, phase coherence of the superconducting order parameter over large scales is required in manifestation of superconductivity, and such phase coherence can easily be affected by scatterings. The gradual degradation of superconductivity was attributed to scattering from roughness at interfaces with the substrate and the covering materials (these other studies were performed ex situ on films covered with a protective layer) (*7*, *9*). On the other hand, our probe is of local nature and is sensitive to the magnitude, rather than the phase, of the order parameter. Moreover, we take special care in the preparation of the substrate, and the Pb film surface is maintained intact in ultrahigh vacuum throughout the measurement stage.

Still, two key questions remain: Why does the T_c drop at 2 ML, and why are the T_c values different for type I and II? We believe that the answer might lie in the fact that even such a pristine film needs to be supported on a substrate. Film-substrate interactions can play an important role in influencing the superconductivity, especially in the 2-ML limit when there is only a single quantum channel of electronic states to support the formation of Cooper pairs or local superconducting ordering. As we described earlier, there are two different atomic arrangements for the 2-ML films: In type I, the underlying 1×1 atomic structure has the same lattice parameter as the bulk Pb, whereas in type II, the $\sqrt{3} \times \sqrt{3}$ atomic structure assumes a similar lattice constant as the Si $\sqrt{3} \times \sqrt{3}$ structure. This result indicates that the type II film is under tensile strain laterally. The phonon spectrum and the interaction of phonons with the electrons should be considerably different (*25*–*27*), resulting in a further reduction of T_c. For films of 4 ML or thicker, the atomic structure is close to the bulk atomic structure. With two or more quantum channels of electronic states to support the formation of Cooper pairs, the effect of substrate can be markedly reduced. If this conjecture is correct, one might be able to fine tune the strength of superconducting ordering in the single-channel limit by engineering the film/substrate interface.

References and Notes

1. M. Strongin, R. S. Thompson, O. F. Kammerer, J. E. Crow, *Phys. Rev. B* **1**, 1078 (1970).
2. G. J. Dolan, J. Silcox, *Phys. Rev. Lett.* **30**, 603 (1973).
3. B. G. Orr, H. M. Jaeger, A. M. Goldman, *Phys. Rev. Lett.* **53**, 2046 (1984).
4. R. C. Dynes, A. E. White, J. M. Graybeal, J. P. Garno, *Phys. Rev. Lett.* **57**, 2195 (1986).
5. D. B. Haviland, Y. Liu, A. M. Goldman, *Phys. Rev. Lett.* **62**, 2180 (1989).
6. A. Yazdani, A. Kapitulnik, *Phys. Rev. Lett.* **74**, 3037 (1995).
7. Y. Guo *et al.*, *Science* **306**, 1915 (2004).
8. D. Eom, S. Qin, M.-Y. Chou, C. K. Shih, *Phys. Rev. Lett.* **96**, 027005 (2006).
9. M. M. Özer, J. R. Thompson, H. H. Weitering, *Nat. Phys.* **2**, 173 (2006).
10. M. M. Özer, Y. Jia, Z. Zhang, J. R. Thompson, H. H. Weitering, *Science* **316**, 1594 (2007).
11. T. Nishio *et al.*, *Phys. Rev. Lett.* **101**, 167001 (2008).
12. A. R. Smith, K.-J. Chao, Q. Niu, C. K. Shih, *Science* **273**, 226 (1996).
13. I. B. Altfeder, K. A. Matveev, D. M. Chen, *Phys. Rev. Lett.* **78**, 2815 (1997).
14. V. Yeh, L. Berbil-Bautista, C. Z. Wang, K. M. Ho, M. C. Tringides, *Phys. Rev. Lett.* **85**, 5158 (2000).
15. W. B. Su *et al.*, *Phys. Rev. Lett.* **86**, 5116 (2001).
16. D.-A. Luh, T. Miller, J. J. Paggel, M. Y. Chou, T.-C. Chiang, *Science* **292**, 1131 (2001).
17. C. M. Wei, M. Y. Chou, *Phys. Rev. B* **66**, 233408 (2002).
18. Z. Zhang, Q. Niu, C. K. Shih, *Phys. Rev. Lett.* **80**, 5381 (1998).
19. Supporting material is available on *Science* Online.
20. E. Ganz, I. Hwang, F. Xiong, S. K. Theiss, J. Golovchenko, *Surf. Sci.* **257**, 259 (1991).
21. T. Schmidt, E. Bauer, *Phys. Rev. B* **62**, 15815 (2000).
22. M. Hupalo, J. Schmalian, M. C. Tringides, *Phys. Rev. Lett.* **90**, 216106 (2003).
23. S. M. Lu *et al.*, *Phys. Rev. B* **75**, 113402 (2007).
24. J. Bardeen, L. N. Cooper, J. R. Schrieffer, *Phys. Rev.* **108**, 1175 (1957).
25. D.-A. Luh, T. Miller, J. J. Paggel, T.-C. Chiang, *Phys. Rev. Lett.* **88**, 256802 (2002).
26. J. J. Paggel, D.-A. Luh, T. Miller, T.-C. Chiang, *Phys. Rev. Lett.* **92**, 186803 (2004).
27. F. Yndurain, M. P. Jigato, *Phys. Rev. Lett.* **100**, 205501 (2008).

28. This work was supported by NSF grant DMR-0606485, the Welch Foundation, and the Texas Advanced Research Program.

Supporting Online Material

www.sciencemag.org/cgi/content/full/1170775/DC1
SOM Text
Fig. S1
References

12 January 2009; accepted 16 April 2009
Published online 30 April 2009;
10.1126/science.1170775
Include this information when citing this paper.